# Electronic Polarizability and Optical Basicity of BaO-B2O3-TeO2 Glass System

**A. Amat** ( azuraida@upnm.edu.my )
Universiti Pertahanan Nasional Malaysia
**M. K. Halimah**
Universiti Putra Malaysia
**M. Ishak**
Malaysian Institute for Nuclear Technology Research (MINT)
**S. N. Nazrin**
Universiti Putra Malaysia
**N. N. Syamimi**
Ostbayerische Technische Hochschule Regensburg
**L. Hasnimulyati**
Universiti Teknologi MARA Cawangan Pahang

**Research Article**

**Keywords:** barium oxide, refractive index, electronic polarizability, optical basicity

**Posted Date:** November 30th, 2021

**DOI:** https://doi.org/10.21203/rs.3.rs-1093838/v1

# Electronic polarizability and optical basicity of $BaO-B_2O_3-TeO_2$ glass system

A. Azuraida[1*], M. K. Halimah[2], M. Ishak[3], S. N. Nazrin[2], N. N. Syamimi[4], L. Hasnimulyati[5]

[1]Department of Physics, Centre for Defence Foundation Studies, Universiti Pertahanan Nasional Malaysia, 57000 Sungai Besi, Kuala Lumpur, Malaysia,

[2]Department of Physics, Faculty of Science, Universiti Putra Malaysia, 43400 Serdang, Selangor, Malaysia.

[3]Technical Support Division, Malaysian Institute for Nuclear Technology Research (MINT), 43000 Bangi, Kajang, Selangor, Malaysia.

[4]Fakultät Angewandte Natur- und Kulturwissenschaften, Ostbayerische Technische Hochschule Regensburg, 93053 Regensburg, Bavaria, Germany.

[5]Faculty of Applied Science, Universiti Teknologi MARA Cawangan Pahang, Kampus Jengka, 26400 Bandar Pusat Jengka, Pahang, Malaysia.

*Correspondence author: azuraida@upnm.edu.my

## Abstract

$[(TeO_2)_{0.7}(B_2O_3)_{0.3}]_{1-x}(BaO)_x$, x = 0.00, 0.05, 0.10, 0.20, 0.25, 0.30 and 0.35 mol fraction glass series were successfully synthesized by conventional melt quenching method. Amorphous phase of all samples was confirmed through X-ray diffraction while optical properties were determined using UV-VIS spectrophotometer. Fourier Transform Infrared (FTIR) analysis showed that the glass structure consisted of $TeO_3$, $TeO_4$, $TeO_6$, $BO_3$ and $BO_4$ structural units. The optical band gap energy, $E_{opt}$ which was calculated from Tauc' plots decreased as the amount of BaO increases, whereas, the Urbach energy value increased. The increase in Urbach energy value was attributed to the increase of defects in glass structure. The refractive indices of glass were found to increase along with the increased amount of BaO, due to the high polarization and high density of host material and glass modifier. The molar polarizability, $\alpha_m$, oxide ion polarizability, $\alpha_o^{2-}$ and optical basicity, $\Lambda$ of the glasses are calculated by Lorentz-Lorenz equation. The glasses were found to possess $\alpha_m$ values between 8.106 – 8.489 $Å^3$, and $\alpha_o^{2-}$ values between 3.303 to 4.772. Meanwhile, optical basicity increases from 0.115 to 0.893.

**Keywords**: barium oxide, refractive index, electronic polarizability, optical basicity

## 1. Introduction

Developments of tellurite glasses began in the early 1950s especially in the optoelectronics field such as fiber optic and laser technology. Tellurite glasses are excellent in glass stability aspect among other oxide glass formers and possess high linear and nonlinear refractive index compared to fluoride and silicate glasses [1-3]. It is also reported that by comparing the density of glasses, the density of tellurite glass falls in the following order: tellurite > germinate > phosphate > silicate [2].

Borate is also one of the most popular glasses which possesses high chemical durability, good solubility of rare earth and easy for synthesisation. In addition, by combining with heavy metal oxide, it is possible to use as an electronic sensor [4], electronic device [5] and radiation shielding material [6-7]. Normally, borate glass consists of $[BO_4]$ and $[BO_3]$ structural units together with non-bridging oxygen when combined with alkali or heavy metal oxide. But it is interchangeable with other $B_xO_y$ structural group [4; 8-9].

Investigation on borotellurite glass system has been growing in recent years. Combination of two glass formers, borate and tellurite is found to affect its physical properties which produces good quality glass. Structural units of $TeO_4$ from tellurite and $BO_4$ from borate have strong tendency to link with each other and produce a high connectivity in glass network. On top of that, suitable ratio of both glass formers will result to a reduction in its hygroscopic nature, while increasing the IR transmission and refractive index [10-12]. However, the number of publications for boro-tellurite glass are still small compared to other glass systems such as silicate, phosphate, boro-silicate, boro-phosphate etc.

In present work, a barium oxide is selected as glass modifier which mixed into the glass composition. The ability of barium composites in sustaining a strong electric field without conducting electricity has been useful as a component of high temperature conductors and electro-ceramics. Due to the non-carcinogenic property of barium, it is not poisonous and does not bio-accumulate. This is a useful perk in glass making industries as it also can increase the refractive index of glass [13, 14, 15].

Therefore, this work offers a new insight for boro-tellurite glass system that focuses on optical properties by adding barium oxide as its glass modifier. The density, structural and optical properties of this glass system are also explored to see their correlations with barium concentration. $B_2O_3$-$TeO_2$ based glass is selected as a glass former due to its low melting temperature, high transparency, and stability against devitrification. In addition, barium tellurite glass with borate is expected to possess high density, high refractive index and large polarizability which lead to the improvement of optical properties, thus making it suitable for photonic devices.

## 2. Methodology

### *2.1 Sample preparation*

A series of glass samples were prepared using melt quenching technique. Tellurium (IV) dioxide ($TeO_2$), Boron oxide ($B_2O_3$) and Barium oxide (BaO) were used to prepare the glasses according to the chemical composition, $[(TeO_2)_{0.7}(B_2O_3)_{0.3}]_{1-x}$ $(BaO)_x$, where the value of x was 0.00, 0.05, 0.10, 0.20, 0.25, 0.30 and 0.35. The chemicals with different composition are mixed together in an agate mortar–pestle and grinded for 30 minutes to obtain fine powder substance, homogenous mixture as well as reducing the formation of air bubbles in the glass sample. The mixed powder was then transferred to an alumina crucible with lid.

Next, the crucible along with the mixed chemical powder were placed inside a furnace with internal temperature of 400°C for 30 minutes at room temperature for a pre-heating process. This process was to decompose the mixture and allow water vapor to evaporate. After 30 minutes of pre-heating, the crucible was transferred immediately to a second furnace for melting process at 900˚C for 50 min. When the mixture in the crucible was completely melted, the molten was then poured into a cylindrical stainless steel split mould which was pre-heated at 400°C. This temperature was achieved empirically through trial and error. If the temperature of the mould was too low, the formed glass will have too much internal stress that will lead to crack and fracture.

The mould was then placed inside the first furnace at 400˚C for 1 hour to eliminate any residual stress in the glass sample. Suitable temperature and time for annealing process were stressed upon to reduce any thermal stresses caused by the quenching process. Afterward, the furnace was turned off. The glass sample was left inside the furnace until the temperature cooled down and achieved room temperature.

*2.2 Sample characterization*

Glass density of all sample are obtained using densimeter with sensitivity of $10^{-3}$ g/cm$^3$ that operated according to Archimedes' principle with distilled water as an immersion liquid. The relation used to calculate density is as follows;

$$\rho = \left(\frac{w_a}{w_a - w_b}\right)(\rho_b) \quad (1)$$

where $w_a$ is weight of sample in air, $w_b$is weight of sample in distilled water and $\rho_b$is density of distilled water.

Molar volume ($V_m$) is the volume occupied by one mole of a substance from a chemical element or a chemical compound at a given temperature and pressure. The molar volume of a glass can be obtained by the relation of;

$$V_m = \left(\frac{M}{\rho}\right) \quad (2)$$

where M is molecular weight of the substances and ρ is the density of glass sample.

The optical properties of the glass samples were determined using UV-Visible Spectrophotometer (UV-VIS) where the electronic polarizability and optical basicity of the glass then can be obtained. When UV-Vis light strikes a sample, the intensity of the light beam is reduced due to reflection and absorption in the sample, and eventually by the scattering of dispersed particles. Before adequate theory was developed, Beer and Lambert have proposed laws on light absorption. Beer's Law states that light absorbed by dilute solutions is proportional to the number of absorbing molecules or the concentration of absorbing molecules. On the other hand, Lambert's Law states that the fraction of radiation absorbed is independent to the intensity of radiation. The combination of these two laws are well-known as the Beer – Lambert's law of the

light absorption which states that the fraction of the incident light absorbed is proportional to the number of molecules in the path. The absorption intensity of an incident light by a glass sample emulates the famous Beer-Lambert's law. In the near absorption edge, the optical absorption coefficient $\alpha(\omega)$ of a glass sample of thickness, t can be calculated from the relation;

$$\alpha(\omega) = \frac{1}{t}\ln\left(\frac{I_o}{I_T}\right) \quad (3)$$

where $\ln(I_o/I_T)$ = absorbance

$I_o$ = intensities of incident light

$I_T$ = intensities of transmitted light.

The band edge is measured using the theory of Davis and Mott in order to obtain values for the optical energy gaps. Davis and Mott found an empirical relation that provided an accurate depiction for the shape of the band edge [15].

$$\alpha(\omega) = A\frac{(\hbar\omega - E_{opt})^r}{\hbar\omega} \quad (4)$$

where α*(ω)* is the frequency dependent optical absorption coefficient, *A* is a fitting constant, $\hbar\omega$ is the reduced Plank constant, $E_{opt}$ is the optical energy gap and *r* is an index derived empirically, in which it could take the value of 2, 3, 1/2 and 3/2 according to the nature of the electronic transition. Al-Ani *et al.,* (1985); Stentz *et al.,* (2000); Prakash *et al.,* (2001) and Murugan *et al.,* (2004) [16-19] had stated that for glass and amorphous material, the best experimental data was at *r = 2*, and the band edge was dominated by indirect transitions. Using r = 2 in Equation (2), the following relation can be attained as:

$$\alpha\hbar\omega^{1/2} = \mathrm{A}(\hbar\omega - E_{opt}) \quad (5)$$

As implied by Equation 2, a plot of $(\alpha\hbar\omega)^{1/2}$ versus $\hbar\omega$ will turn out as a straight line in the vicinity of the band edge. Furthermore, the x-intercept of this line will be the value of $E_{opt}$.

In the case of glasses and any amorphous materials, a band tail exists in the forbidden energy band gap. The extent of band tailing is a measurement of the material disorder and is estimated by Urbach rule [20]. For fundamental absorption edge in lower incident photon energy $(\hbar\omega)$ between $10^2$-$10^4$ $cm^{-1}$, the absorption coefficient $\alpha(\omega)$ follows Urbach law given by;

$$\alpha(\omega) = B\ exp\left(\frac{\hbar\omega}{\Delta E}\right) \quad (6)$$

where B is a constant and $\Delta E$ is the Urbach's energy. The Urbach energy values are determined from the slopes of linear region of the plots in ln $\alpha(\omega)$ vs $\hbar\omega$. The values of wavelength correspond to the absorption edge, where the intensity reaches the maximum value in optical absorption spectra is taken as cut-off wavelengths, $\lambda_{cut\text{-}off}$.

The refractive indices, noted as n, for the glass samples are appraised from the optical band gap values using the relation put forward by Dimitrov and Sakka (1996) and Eraiah (2006) [21-22].

$$\frac{n^2-1}{n^2+2} = 1 - \sqrt{\frac{E_{opt}}{20}} \tag{7}$$

The quoted refractive index values correspond to the respective $E_{opt}$ values of the present glass samples. However, there are chances of small errors creeping into the process of estimating the n using the value of $E_{opt}$, owing to the extrapolation of $(\alpha\hbar\omega)^{1/2}$ vs $(\hbar\omega)$ plots.

The average molar refraction, $R_m$ of the glasses is taken from the Lorentz-Lorenz equation [23].

$$R_m = \left[\frac{n^2-1}{n^2+2}\right]\frac{M}{\rho} = \left[\frac{n^2-1}{n^2+2}\right]V_M \tag{8}$$

where the quantity of $[(n^2-1)/(n^2+2)]$ refers to reflection loss, M is molecular weight, ρ is density and $V_m$ is the molar volume. This parameter is able to give an insight on the contribution of ionic packing in controlling the general refractive index of the glass. Besides that, it is also directly proportional to the polarizability of the constituent ions used in a glass system.

There are two types of polarizabilities that can be calculated which are molar polarizability and oxide ion polarizability. Molar polarizability is defined as the total polarizability of a mole of a substance, which relies on temperature, pressure, and refractive index. According to the Clausius-Mosotti relation, molar polarizability of the materials $(\alpha_m)$ is given by the relation:

$$\alpha_m = \left[\frac{3}{4\pi N}\right] R_m \tag{9}$$

where N is the Avogadro's number. On the other hands, the polarizability of oxide ions $\alpha_o{}^{2-}$ has been calculated using the equation proposed by Dimitrov and Sakka, (1996) [21].

$$\alpha_o{}^{2-} = \left[\frac{R_M}{2.52} - \sum \alpha_i\right](N_{o^{2-}})^{-1} \quad (10)$$

where $\sum \alpha_i =$ molar cation polarizability

$N_{o^{2-}}$ = the number of oxide ions in the chemical formula.

Based on the data of $\alpha_o{}^{2-}$, the parameter that can be determined is optical basicity. The level of acidity or basicity of glass can be said to relate to the electron donor power of oxygen atom. Oxides with low electron donating power and high chemical hardness are called as acid. On the other hand, oxides with higher electron donating power and weaker chemical hardness are considered as bases. Referring to Elkhoshkhany *et al*., (2014) [24], in the instances where the optical basicity of an oxidic medium increased, it is an indication that there is a decreasing covalency in the cation-oxygen bonding. For various oxide ions Duffy, (1989) [25] had suggested the following relation between oxide ion polarizability, $\alpha_o{}^{2-}$ and optical basicity, $\Lambda$ [23]:

$$\Lambda = 1.67\left(1 - \frac{1}{\alpha_o{}^{2-}}\right) \quad (11)$$

## 3.0 Result and Discussion

### *3.1 Density and molar volume*

All glasses prepared in this work were transparent and clear from air bubbles. The addition of BaO content in $(TeO_2)_{0.7}(B_2O_3)_{0.3}$ glass system changed the colour tone from colourless to light-green.

Density is the key concept in analysing the structure of glasses, relying on the number and type of atoms as well as atom combination bonding [26]. It can be defined as the degree of compactness of a substance or glass structure. The densities values of all samples were listed in Table 1. It had been revealed that the density of glass system increased with increased in BaO concentration. As expected, the small increment of this glass density was due to the replacement of lighter density of $TeO_2$ (5.67 $gcm^{-3}$) and $B_2O_3$ (2.46 $gcm^{-3}$) in comparison to BaO (5.72 $gcm^{-3}$). In addition, Manikandan *et al*., (2012) [27] had stated that BaO had a tendency to strengthen the three-

dimensional nature of the glass network and made the glass denser. The achieved density in the present work was similar to the density value of $0.4BaO\text{-}0.6B_2O_3$ glass (3.38 $gcm^{-3}$) and $35.8BaO\text{-}64.2B_2O_3$ (3.61 $gcm^{-3}$) which were prepared by Kapoor *et al*., (2000) and Warner and Rawson, (1978) [28-29], respectively. Meanwhile, Desirena *et al*., (2009) [30] reported that the density of $20BaO–10Cs_2CO_3 –70TeO_3$ glass was 4.733 $gcm^{-3}$, which was higher than the density observed in this work. Furthermore, Ghada (2018) [31] stated that the increment of density in the glass system also was probably caused by an increment in the number of non-bridging oxygen (NBO) atoms. Besides, the introduction of modifier barium ions will attempt to occupy the interstices within the network and contribute to the creation of a more compact glass.

**Table 1** Density, molar volume and average boron-boron separation for all glasses

| **Glass sample** | **Density, ρ ($gcm^{-3}$)** | **Molar volume, $V_m$ ($cm^3\ mol^{-1}$)** | **$\langle d_{B\text{-}B} \rangle$ (nm)** |
|---|---|---|---|
| BTe-0Ba | 3.17 | 40.86 | 0.4003 |
| BTe-0.05Ba | 3.28 | 39.97 | 0.4054 |
| BTe-0.10Ba | 3.38 | 39.85 | 0.3823 |
| BTe-0.15Ba | 3.46 | 39.31 | 0.3620 |
| BTe-0.20Ba | 3.50 | 39.14 | 0.3619 |
| BTe-0.25Ba | 3.59 | 38.43 | 0.3536 |
| BTe-0.30Ba | 3.63 | 38.20 | 0.3411 |
| BTe-0.35Ba | 3.69 | 38.10 | 0.3299 |

Molar volume can be described as the volume occupied by a unit mass of the glass samples. This parameter also can be used as a numerical guideline to recognize an open structure in a glass structure. Therefore, the sample with the highest molar volume corresponds to the maximum open structure [32]. Typically, molar volume and density shows an opposite behaviour. Based on the data recorded in Table 1, the similar case also occurs in this study. In present work, the density of glass system increased while molar volume decreased as BaO content increased. The trend of this result followed the relationship between density and molar volume as shown in Equation (2), which is the inversely proportional relation between density and molar volume. The decreasing molar volume might be caused by the decreasing bond length and the space between atoms in a

glass network. This process then affected the compactness of the glass network. This behaviour also can be observed in BaO borate glass explained by Obayes *et al*., (2016) [33]. It was stated that the addition of BaO (20 to 60 mol%) in MgO –$Na_2O$ – $B_2O_3$ glass system reduced average boron-boron separation ($d_{B\text{-}B}$) from ~0.415 nm to ~0.333 nm, and thus, yielded a compact glass.

In order to confirm the increase in the compactness of the glass structure after addition of glass modifier, the average boron–boron separation, $\langle d_{B\text{-}B} \rangle$ had been calculated and also listed in Table 1. The average boron-boron separation $\langle d_{B\text{-}B} \rangle$ was calculated using the equation;

$$\langle d_{B-B} \rangle = \left( \frac{V_m^B}{N_A} \right)^{1/3} \tag{12}$$

where $N_A$ was Avogadro's number (6.0228 × $10^{23}$ g/mol) and $V_m^B$ was the volume which corresponded to the volume that contained one mole of boron within the given structure. This volume, $V_m^B$ was determined using the following relation;

$$V_m^B = \frac{V_m}{2(1 - x_B)} \tag{13}$$

where $x_B$ was the molar fraction of boron oxide, $B_2O_3$ and $V_m$ was the molar volume of glass.

The average boron-boron separation $\langle d_{B\text{-}B} \rangle$ was calculated to give clearer understanding in the modification of glass network due to the addition of BaO. Boron atoms were the central atoms with negatively charged tetrahedral - $BO_{4/2}$ units [34]. Since $V_m^B$ depended on cation species, the calculated values of average boron-boron separation $\langle d_{B\text{-}B} \rangle$ decreased with the increase in the BaO contents in the glass system as shown in Table 1. Thus, the incorporation of $V_m^B$ on expense of $B_2O_3$ led to a significant contraction of the glass structural network which confirmed the obtained density and molar volume values [35].

### *3.2 Structural Properties*

#### *3.2.1 XRD analysis*

Figure 1 displayed the example of X-ray diffraction pattern for BTe-0.25BaO glass and similar patterns also recorded by the other glass samples in this study. There was no sharp peak representing the crystal structure in the XRD spectra. This graph mainly showed the presence of

broad diffuse scattering around 2θ ≅ 24-30˚. Similar pattern of XRD graph also shown in multi-composition borotellurite glasses which were reported by Hasnimulyati *et al*., (2016) and Nazrin *et al*., (2021) [36-37]. Due to the absence of a sharp peak, it can be inferred that there was no long range order in atomic arrangements thus ensures the glass had an amorphous structure.

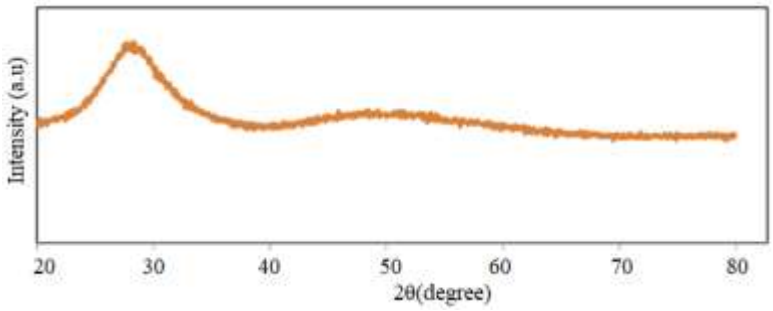


**Fig. 1.** XRD spectrum of BTe-0.25BaO glass

### *3.2.2 FTIR analysis*

The FTIR spectra for present glass samples were plotted in Figure 2. There are six main absorptions peak: (1) band shoulder at 790 $cm^{-1}$, (2) three weak peaks at intensities of ~430 $cm^{-1}$, 535 $cm^{-1}$ and ~1043 $cm^{-1}$, and (3) two broad band at 1200 $cm^{-1}$ and 1300 $cm^{-1}$. The broad band of 1300 $cm^{-1}$ decreased slowly whereas the band centred at 1200 $cm^{-1}$ increased, followed by the presence of new narrow absorption peak around 840 and 1200 $cm^{-1}$ with increasing amount of barium oxide. These assigned to the existence of B–O bond stretching vibrations of $BO_3$ units from boroxol rings and boroxyl groups [38]. The weak absorption peak at about 1043 $cm^{-1}$ was due to the stretching vibration of B-O bond from tetrahedral $BO_4$ units [39] and peak occurred near 535 $cm^{-1}$ due to B-O-B vibration overlap with $TeO_4$ polyhedron. The shoulder band at 790 $cm^{-1}$ was due to the stretching vibration of B-O-B in $B_3O_6$ boroxol rings overlapping with Te-O bond with non-bridging oxygen [38]. In the meantime, the FTIR absorption band located around 760-790 $cm^{-1}$ might be contributed by: (i) stretching vibrations of short Te-O bonds with non-bridging oxygen atoms in $O_3Te\text{-}O^-$ groups (ii) stretching vibration of Te=O double bonds in $O_2Te{=}O$ groups, and (iii) stretching vibrations of long Te-O bonds with non-bridging oxygen atoms in $O_3Te\text{-}O^-$ groups [40].

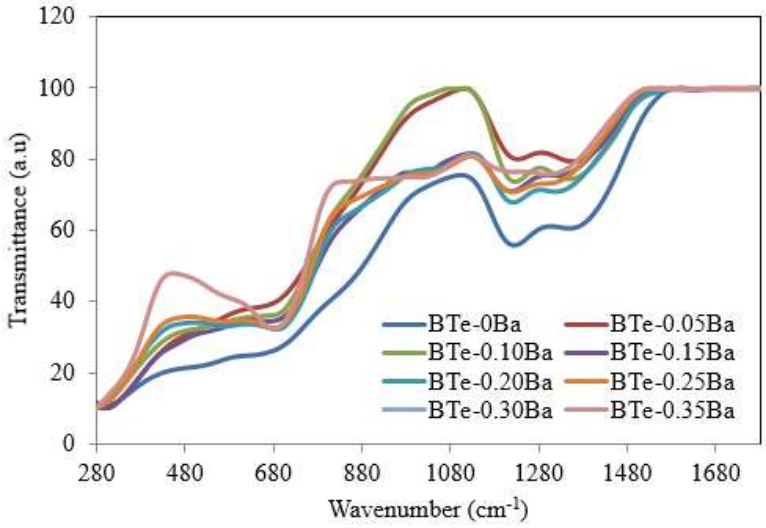


**Fig. 2.** FTIR spectra of all glasses with increment in BaO concentration

It can be observed that by increasing BaO concentration, the intensity of absorption band located around 430 $cm^{-1}$ are getting lesser. This behaviour might be due to increasing distraction in glass network which affected the alterations of bond angles and/or bond lengths. According to Saeed et al., (2018) [41], the absorption band located ~430 $cm^{-1}$ attribute to the bending vibration of Te – O – Te or/and O – Te – O. Furthermore, the characteristic band of BaO is also observed around 862 $cm^{-1}$. The FTIR profile unveils that the presence of both $BO_3$ and $BO_4$ structural units for borate appeared in the specific region. In the region of 850–1100 $cm^{-1}$, bands appeared due to the stretching of B–O bond in tetrahedral $BO_4$ units, which are the vibrations of tetra borate groups of $BO_4$ units. Bands in the region from 1150 to 1456 $cm^{-1}$ are generally due to B–O bond stretching in trigonal $BO_3$ units. The band centred between 900 and 1100 $cm^{-1}$ are attribute to the presence of boron atom in tetrahedral coordination, $BO_4$ units.

### *3.3 Optical Properties*

Optical absorption spectra of all glasses are measured for the wavelength in range of 220 – 800 nm. The optical absorption for BTe-0.25BaO glass are illustrated in Figure 3. A cutoff wavelength was found to shift towards higher wavelength when BaO was inserted into the glass system. Addition of BaO content in $(TeO_2)_{0.7}(B_2O_3)_{0.3}$ glass system was believed to increase the

non-bridging oxygen atoms into glass structure, thus resulting in cutoff wavelength towards higher wavelength.

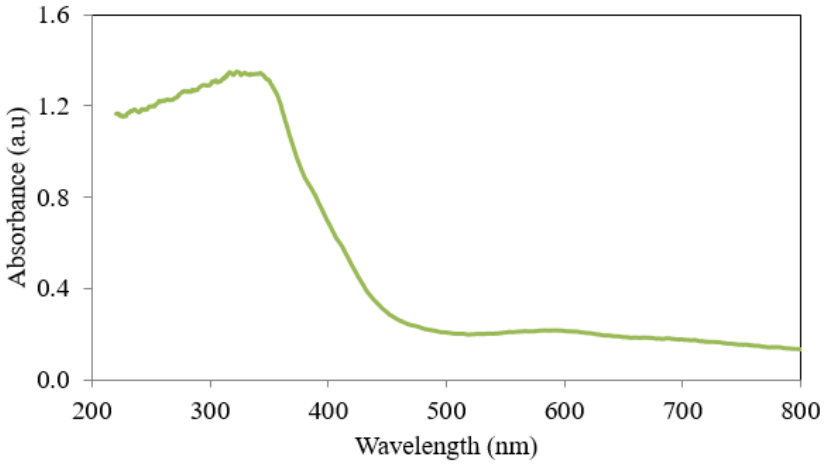


**Fig. 3.** Optical absorption for BTe-0.25BaO glass

The variation of the optical band gap $E_{opt}$ for this glass series as listed in Table 2 determined from the data in Figure 3 and calculated by using Equation (3) – (6). Both direct and indirect transitions showed a decreasing pattern with increasing amount of BaO. In addition, the values of band gap in direct transition (3.15 - 3.52 eV) were higher than that of indirect transition (2.39 - 2.89 eV). The increasing number of NBOs was one of the reasons that contributed to the decrement in band gap value. In oxide glasses, the non-bridging oxygens had higher magnitude of negative charges than that on the bridging oxygens. To increase the ionicity of oxygen atoms, the bridging oxygen was converted to non-bridging oxygen ions, which raised the top of the valence band, leading to the reduction of band gap [42]. The Urbach energy, ΔE for $[(TeO_2)_{0.7}(B_2O_3)_{0.3}]_{1-x}(BaO)_x$ glass system was presented in the Table 2. The values increased from 0.611–0.904 eV as BaO content increased, which was believed to indicate a more structural disorder. As formerly reported by Insitipong *et al*., (2011) [5], it is suggested that the degree of disorder in borate based glass is present in various borate groups. Lower value of Urbach energy had been reported by Bahadur *et al*., (2010) [43] for barium - fluorotellurite glass. The low value indicated there was minimum defects that present in the glass, which meant that the glass was stable and highly homogeneous.

**Table 2** Optical band gap, $E_{opt}$ and Urbach energy, ΔE values for all samples

| Glass sample | $E_{opt,direct}$ (eV) | $E_{opt,indirect}$ (eV) | ΔE (eV) |
|---|---|---|---|
| BTe-0Ba | 3.52 | 2.89 | 0.611 |
| BTe-0.05Ba | 3.49 | 2.90 | 0.609 |
| BTe-0.10Ba | 3.46 | 2.68 | 0.634 |
| BTe-0.15Ba | 3.43 | 2.66 | 0.766 |
| BTe-0.20Ba | 3.24 | 2.57 | 0.862 |
| BTe-0.25Ba | 3.23 | 2.46 | 0.898 |
| BTe-0.30Ba | 3.20 | 2.44 | 0.899 |
| BTe-0.35Ba | 3.15 | 2.39 | 0.904 |

The refractive index, n of $[(TeO_2)_{0.7}(B_2O_3)_{0.3}]_{1-x}(BaO)_x$ glass system in this work generally increased from 1.783 to 1.826 as BaO content increased up to 0.35 molar fraction. The increasing value of n was due to the increasing value of their glass density. Besides, the non-bridging oxygen can affect the polarizability of the ions which may lead to a change in the refractive index. The increasing number of non-bridging oxygen was attributed to the conversion of $TeO_4$ trigonal bipyramid to $TeO_3$ trigonal pyramid which will increase both the polarizability and refractive index simultaneously [44]. Molar refraction, $R_m$ and oxide ion polarizability, $\alpha_o^{2-}$ values were strongly related with the value of refractive index and molar volume. By using the equation provided in last section (Equation 8 and 10), the $R_m$ value for $[(TeO_2)_{0.7}(B_2O_3)_{0.3}]_{1-x}(BaO)_x$ glass was found to increase from 15.222 to 16.567 while $\alpha_o^{2-}$ values increased from 3.303 to 4.772 $Å^3$ as BaO content increased in the glass system. The increase of $\alpha_o^{2-}$ value then caused the increment of optical basicity, Λ value of the glass samples.

**Table 3** Refractive index (n), molar refraction ($R_m$), molar polarizability ($\alpha_m$), oxide ion polarizability ($\alpha_o^{2-}$), optical basicity (Λ) and metallization criterion (M) for all samples.

| Glass code | n | $R_m$ | $\alpha_m$ ($Å^3$) | $\alpha_o^{2-}$ ($Å^3$) | Λ | M |
|---|---|---|---|---|---|---|
| BTe-0Ba | 1.783 | 15.222 | 8.106 | 3.303 | 0.115 | 0.430 |
| BTe-0.05Ba | 1.781 | 15.112 | 8.110 | 3.417 | 0.833 | 0.437 |
| BTe-0.10Ba | 1.786 | 15.345 | 8.119 | 3.572 | 0.841 | 0.421 |
| BTe-0.15Ba | 1.801 | 15.465 | 8.127 | 3.722 | 0.852 | 0.403 |
| BTe-0.20Ba | 1.803 | 15.988 | 8.246 | 3.893 | 0.871 | 0.399 |

| | | | | | | |
|---|---|---|---|---|---|---|
| BTe-0.25Ba | 1.839 | 16.452 | 8.412 | 4.251 | 0.888 | 0.379 |
| BTe-0.30Ba | 1.832 | 16.388 | 8.439 | 4.540 | 0.891 | 0.361 |
| BTe-0.35Ba | 1.826 | 16.567 | 8.489 | 4.772 | 0.893 | 0.355 |

Halimah *et al*., (2017) [45] had proposed that metallization criterion can be used to determine the propensity for metallization and to investigate the insulating behaviour of the fabricated glasses. Metallization criterion, M of present glass samples had been calculated using equation;

$$M = 1 - \frac{R_m}{V_m} \tag{14}$$

where $R_m$ is molar refraction and $V_m$ is molar volume. The necessary and sufficient conditions for predicting nonmetallic or metallic character of solids were: $R_m/V_m > 1$, for metal and $R_m/V_m < 1$, for nonmetal. Oxides with good nonlinear optical properties possessed a metallization criterion of approximately 0.30–0.45 [46]. From previous work, the metallization criterion for most of the tellurite glasses could exist in the range of 0.35–0.45, where glasses with metallization criterion approaching 1 are known as insulator. Meanwhile, Saeed et al., (2018) [41] stated that the metallization values of less than 1 defines that the width of both valence and conduction bands becomes large.

The decrease in value of metallization criterion was discovered in $[(TeO_2)_{0.7}(B_2O_3)_{0.3}]_{1-x}(BaO)_x$ glass series with increasing amount of BaO. The decrement (0.430 to 0.355) was attributed to the increase of the refractive index of glasses and the decrease in the band gap energy. The small value of metallization criterion (<0.5) meant that the width of both conduction and valence bands became larger, resulting in a narrower band gap and increase in metallicity of the solid material [47]. Besides, the range value of metallization criterion also indicated that this glass samples could be the best material for non-linear application compared to other glasses.

Hence, it can inferred that as barium oxide glass is known for its high refractive index, hardness and stability as well as low dispersion, barium oxide glass is known to have a good optical performance. It has a high potential to be used in the production of a desirable multifocal ophthalmic lens, which formed by fusing a glass segment of high refractive index onto a glass

blank of lower refractive index. In the process, the glass used in the segment shall preferably have a relatively high refractive index in order to reduce the thickness of the lens [48].

## Conclusion

A series of $[(TeO_2)_{0.7}(B_2O_3)_{0.3}]_{1-x}(BaO)_x$ glass system had been successfully synthesized. Density results illustrate the increment in the compactness of the structure with the addition of BaO. From FTIR analysis, most of the glass samples consisted of $TeO_3$, $TeO_4$, $BO_3$ and $BO_4$ structural units. By adding BaO in glass system, the increment of non-bridging oxygen atoms can be found. The fundamental absorption edge shifted to a higher wavelength when BaO concentration increased. The shift of fundamental absorption edge was most likely related to structural rearrangement between the modifier and glass network. The optical band gap, $E_{opt}$ of $[(TeO_2)_{0.7}(B_2O_3)_{0.3}]_{1-x}(BaO)_x$ glasses was found to decrease with the increasing amount of BaO. The decrease in optical band gap was discussed on the basis of the glass network expansion and the subsequent formation of non-bridging oxygen atoms. The value of Urbach energy was found to be opposite with optical band gap value. The increase in Urbach energy value was attributed to the increasing disorder-ness of glass structure. Glasses with high value of Urbach energy will have greater tendency to convert weak bonds into defects. The increase in refractive index value was due to the increasing concentration of glass modifier and was also affected by the increment in both electronic polarizability and optical basicity.

## Acknowledgement

The authors appreciate the financial support for the work from Universiti Pertahanan Nasional with Short Term Grant UPNM/2019/GPJP/2/SG/6.

## Author contributions

All authors contributed equally to the paper.

## Declarations

**Conflicts of interest**: There is no conflict of interest.

## References

[1] V. V. Dorofeev, A. N. Moiseev, M. F. Churbanov, G. E. Snopatin, A. V. Chilyasov, I. A. Kraev, E. M. Dianov, High-purity $TeO_2$–$WO_3$– ($La_2O_3$, $Bi_2O_3$) glasses for fiber-optics. Opt. Mater. 33(12) (2011) 1911-1915.

[2] R. El-Malawany, Tellurite glasses, Physical properties and data, CRC Press LLC, Bota Racon, Florida, 2002.

[3] J. S. Wang, E. M. Vogel, E. Snitzer, Tellurite glass: a new candidate for fiber devices. Opt. Mater. 3(3) (1994) 187-203.

[4] N. M. Bobkova, Properties and structure of bismuth-borate glasses. Glass Ceram+. 72(9-10) (2016) 360-365.

[5] S. Insitipong, J. Kaewkhao, T. Ratana, P. Limsuwan, Optical and structural investigation of bismuth borate glasses doped with $Dy^{3+}$. Procedia Eng. 8 (2011) 195-199.

[6] K. Kirdsiri, J. Kaewkhao, A. Pokaipisit, W. Chewpraditkul, P. Limsuwan, Gamma-rays shielding properties of xPbO:(100− x) $B_2O_3$ glasses system at 662 keV. Ann. Nucl. Energy. 36(9) (2009) 1360-1365.

[7] S. Y. Marzouk, F. H. Elbatal, Infrared and UV–visible spectroscopic studies of gamma-irradiated $Sb_2O_3$–$B_2O_3$ glasses. J. Mol. Struct. 1063 (2014) 328-335.

[8] S. R. Rejisha, N. Santha, Structural investigations on 20MO-x$Bi_2O_3$-(80-x) $B_2O_3$ (M= Ca, Sr and Ba; x= 15 and 55) glasses. J. Non. Cryst. Solids. 357(22-23) (2011) 3813-3821.

[9] E. I. Kamitsos, G. D. Chryssikos, Borate glass structure by raman and infrared spectroscopies. J. Mol. Struct. 247 (1991) 1-16.

[10] H. Bürger, W. Vogel, V. Kozhukharov, M. Marinov, Phase equilibrium, glass-forming, properties and structure of glasses in the $TeO_2$-$B_2O_3$ system. J. Mater. Sci. 19(2) (1984) 403-412.

[11] R. Kaur, S. Singh, O. P. Pandey, UV–VIS spectroscopic studies of gamma irradiated lead sodium borosilicate glasses. J. Mol. Struct. 1060 (2014) 251-255.

[12] M. K. Halimah, W. M. Daud, H. A. A. Sidek, A. S. Zainal, A. H. Zainul, H. Jumiah, Structural analysis of borotellurite glass. Am. J. Appl. Sci. 5 (2007) 323-327.

[13] A. Azuraida, M. K. Halimah, H. A. A. Sidek, C. A. C. Azurahanim, S. M. Iskandar, M. Ishak, A. Nurazlin, Comparative studies of bismuth and barium boro-tellurite glass system: structural and optical properties. Chalcogenide Lett. 12(10) (2015) 497-503.

[14] J. Partyka, K. Gasek, K. Pasiut, M. Gajek, Effect of addition of BaO on sintering of glass–ceramic materials from $SiO_2$–$Al_2O_2$–$Na_2O$–$K_2O$–CaO/MgO system. J. Therm. Anal. Calorim. 125(3) (2016) 1095-1103.

[15] E. A. Davis, N. Mott, Conduction in non-crystalline systems V. Conductivity, optical absorption and photoconductivity in amorphous semiconductors. Philos. Mag. 22(179) (1970) 0903-0922.

[16] S. K. J. Al-Ani, C. A. Hogarth, R. A. El-Malawany, A study of optical absorption in tellurite and tungsten-tellurite glasses. J. Mater. Sci. 20(2) (1985) 661-667.

[17] D. Stentz, H. B. George, S. E. Feller, M. Affatigato, Comparison of the optical cutoffs of bismuth borate and bismuth germanate glasses. Phys. Chem. Glasses. 41(6) (2000) 406-408.

[18] G. V. Prakash, D. N. Rao, A. K. Bhatnagar, Linear optical properties of niobium-based tellurite glasses. Solid State Commun. 119(1) (2001) 39-44.

[19] G. S. Murugan, Y. Ohishi, $TeO_2$–BaO–SrO–$Nb_2O_5$ glasses: a new glass system for waveguide devices applications. J. Non. Cryst. Solids. 341(1-3) (2004) 86-92.

[20] S. Manning, *A study of tellurite glasses for electro-optic optical fibre devices* (Doctoral dissertation). The University of Adelaide. 2011

[21] V. Dimitrov, S. Sakka, Electronic oxide polarizability and optical basicity of simple oxides. J. Appl. Phys. 79(3) (1996) 1736-1740.

[22] B. Eraiah, Optical properties of samarium doped zinc-tellurite glasses. Bull. Mater. Sci. 29(4) (2006) 375-378.

[23] Y. B. Saddeek, K. A. Aly, S. A. Bashier, Optical study of lead borosilicate glasses. Physica B Condens. Matter. 405(10) (2010) 2407-2412.

[24] N. Elkhoshkhany, R. Abbas, R. El-Mallawany, A. J. Fraih, Optical properties of quaternary $TeO_2$–ZnO–$Nb_2O_5$–$Gd_2O_3$ glasses. Ceram. Int. 40(9) (2014)14477-14481.

[25] J. A. Duffy, Electronic polarizability and related properties of the oxide ion. Phys. Chem. Glasses. 30(1) (1989) 1-4.

[26] A. Q. Tool, L. W., Tilton, J. B. Saunders, Changes caused in the refractivity and density of glass by annealing. J. Res. Natl. Bur. Std. 38 (1947) 519-26.

[27] N. Manikandan, A. Ryasnyanskiy, J. Toulouse, Thermal and optical properties of $TeO_2$–ZnO–BaO glasses. J. Non. Cryst. Solids. 358(5) (2012) 947-951.

[28] S. Kapoor, H. B. George, A. Betzen, M. Affatigato, S. Feller, Physical properties of barium borate glasses determined over a wide range of compositions. J. Non. Cryst. Solids. 270(1-3) (2000) 215-222.

[29] D. Warner, H. Rawson, The effect of glass composition on the mean dispersion of barium borate glasses. J. Non. Cryst. Solids. *29*(2) (1978) 231-237.

[30] H. Desirena, A. Schülzgen, S. Sabet, G. Ramos-Ortiz, E. De la Rosa, N. Peyghambarian, Effect of alkali metal oxides $R_2O$ (R= Li, Na, K, Rb and Cs) and network intermediate MO (M= Zn, Mg, Ba and Pb) in tellurite glasses. Opt. Mater. 31(6) (2009) 784-789.

[31] Ghada A. Optical properties of $[(TeO_2)_{0.7}(B_2O_3)_{0.3}]_{100-x}(BaO)_x$ glass system. Al Azhar Bull. Sci. 29 (2) (December) (2018) 7-11.

[32] S. M. Iskandar, M. K. Halimah, W. M. D. W. Yusoff, H.A.A. Sidek, A. R. Azhar, Structural and optical properties of lead-boro-tellurite glasses induced by gamma-ray. Int. J. Mol. Sci. 14 (2013) 3201–3214.

[33] H. K. Obayes, H. Wagiran, R. Hussin, M. A. Saeed, Structural and optical properties of strontium/copper co-doped lithium borate glass system. Mater. Des. 94 (2016) 121-131.

[34] G. P. Singh, P. Kaur, S. Kaur, D. P. Singh, Gamma ray effect on the covalent behaviour of the $CeO_2$–BaO–$B_2O_3$ glasses. Physica B Condens. Matter. 450 (2014) 106-110.

[35] S. Ibrahim, M. M. Gomaa, H. Darwish, Influence of $Fe_2O_3$ on the physical, structural and electrical properties of sodium lead borate glasses. J. Adv. Ceram. 3(2) (2014) 155-164.

[36] L. Hasnimulyati, M. K. Halimah, A. Zakaria, S. A. Halim, M. Ishak, C. Eevon, Structural and optical properties of $Tm_2O_3$-doped zinc borotellurite glass system. J. Ovonic Res. 12(6) (2016) 291-299.

[37] S. N. Nazrin, M. K. Halimah, F. D. Muhammad, A. A. Latif, S. M. Iskandar, A. S. Asyikin, Experimental and theoretical models of elastic properties of erbium-doped zinc tellurite glass system for potential fiber optic application. Mater. Chem. Phys. 259 (2021)123992.

[38] H.A. Othman, H.S. Elkholy, I.Z. Hager, FTIR of binary lead borate glass: Structural investigation. J. Mol. Struct. 1106 (2016) 286-290.

[39] A. Abou Shama, F. H. El-Batal, Structural analysis of glassy lead borate containing $MoO_3$ in relation to its optical properties. Egypt. J. Solids, 29 (1) (2006) 49-67.

[40] V. O. Sokolov, V. G. Plotnichenko, V. V. Koltashev, Structure of barium chloride-oxide tellurite glasses. J. Non. Cryst. Solids. 355(31-33) (2009) 1574-1584.

[41] A. Saeed, Y. H. Elbashar, S. U. El Khameesy, A novel barium borate glasses for optical applications. Silicon, 10(2) (2018) 569-574.

[42] I. Kabalci, J. Zheng, L. Wang, L. Tan, Y. Xue, Z. Zhang, M. Peng, Novel compositions of $Bi_2O_3$-ZnO-$TeO_2$ glasses: Structure and hardness analysis. J. Non. Cryst. Solids. 464 (2017) 23-29.

[43] A. Bahadur, Y. Dwivedi, S. B. Rai, Spectroscopic study of Er: Sm doped barium fluorotellurite glass. Spectrochim. Acta A Mol. Biomol. *77*(1) (2010)101-106.

[44] M. K. Halimah, S. N. Nazrin, F. D. Muhammad, Influence of silver oxide on structural, physical, elastic and optical properties of zinc tellurite glass system for optical application. Chalcogenide Lett. 16(8) (2019) 365 – 385.

[45] M. K. Halimah, M. F. Faznny, M. N. Azlan, H. A. A. Sidek, Optical basicity and electronic polarizability of zinc borotellurite glass doped $La^{3+}$ ions. Results Phys. 7 (2017) 581-589.

[46] Y. Wang, S. Dai, F. Chen, T. Xu, Q. Nie, Physical properties and optical band gap of new tellurite glasses within the $TeO_2$–$Nb_2O_5$–$Bi_2O_3$ system. Mater. Chem. Phys. 113(1) (2009) 407-411.

[47] B. Bhatia, S. L. Meena, V. Parihar, M. Poonia, Optical basicity and polarizability of $Nd^{3+}$-doped bismuth borate glasses. New J. Glass Ceram. 5(03) (2015) 44.

[48] BASE, P. O. T. A. W. UNITED STATES “PATENT OFFICE.